Journal of Physics: Conference Series

Defect investigations of an iron-nickel meteorite

To cite this article: P Parz *et al* 2013 *J. Phys.: Conf. Ser.* **443** 012032

Defect investigations of an iron-nickel meteorite

P Parz[1], M Leitner[1], W Sprengel[1], H Reingruber[2], and W Puff[1]

[1]Graz University of Technology, Institute of Materials Physics, Petersgasse 16, 8010 Graz, AUSTRIA

[2]Institute for Electron Microscopy, Graz University of Technology, and Center for Electron Microscopy Graz, Steyrergasse 17, A-8010 Graz, Austria

E-mail: p.parz@tugraz.at

Abstract. A sample from the Gibeon meteorite, an iron-nickel meteorite with the typical two-phase Widmanstätten structure, was investigated by positron annihilation techniques. A high mean positron lifetime was observed which derives from open volume defects. The meteorite samples were then gradually heated in a high-vacuum furnace and cooled down to room temperature. Upon temperature treatment a decrease of the mean positron lifetime was observed, as well as a gradual evolution of the 2-dimensional Doppler broadening spectra towards pure iron. This leads to the conclusion that the open volume defects are formed during slow cooling in the progress of the formation of the Widmanstätten structure. Upon re-heating these defects start to dissolve and do not re-appear due to fast cooling rates. We therefore attribute the open volume defects to misfit dislocations between the Kamacite (Ni-poor) and Taenite (Ni-rich) phases.

1. Introduction

Iron-nickel meteorites are well known for their unique microstructure. Due to their very low cooling rates in space a coarse grained structure, the so-called Widmanstätten pattern is formed [1]. This low cooling rate precludes the reproduction of this unique pattern in laboratory. Therefore, the meteorite sample was expected to be in thermodynamic equilibrium and free of defects. The aim of this study was to verify this condition by positron annihilation.

2. Materials and Methods

The meteorite sample with a composition of Ni 7.93 wt.-%, Co 0.41 wt.-%, P 0.04 wt.-%, 91.62 wt.-% Fe and small amounts of carbon [1] was cut into pieces of approximately $8\times8\times3$ mm^3 with a low-speed diamond saw. Upon its journey through space the meteorite was subject to very low cooling rates, of approximately 35 K per one million years [2]. The unique cooling rates are the reason for the typical Widmanstätten structure, a two-phase microstructure of Fe-rich Kamacite (ferrite, α-iron) and Ni-rich Taenite (austenite, γ-iron). The meteorite samples were measured at room temperature and subsequent subject to thermal treatment.

Studies of positron lifetime and two-dimensional Doppler broadening (2d-DB) were performed in the same manner as described recently [3]. Summarizing briefly, a conventional fast-fast spectrometer setup with a time resolution of 230 ps full width at half maximum (FWHM) was used for positron lifetime measurements. From the measured positron lifetime spectra ($>5\times10^6$ counts) the mean positron lifetime is derived. Since the focus of this work is on 2d-DB, a detailed lifetime component analysis is not included**.** The 2d-DB measurements were performed in a coincidence setup of two high-purity Ge detectors with an energy resolution of the two detector system of 0.88 keV (FWHM) related to the 511 keV γ-line. A peak-to-background ratio of ~8×10^5 was achieved, which ensured sensitivity to annihilation events with high momentum (core) electrons. Two-dimensional spectra with an energy width of ~1 keV per channel and (6 to 8)$\times10^7$ counts were collected, from which the background-free Doppler spectra were obtained. All measurements were performed at room temperature. The 2d-DB spectra were presented and analyzed in the following two ways in order to cross check the reliability of the obtained results.

For a numerical analysis, the 2d-DB spectra were fitted by a weighted linear combination of the spectra measured on pure undeformed and deformed elements following Somoza et al. [4]:

$$S = f_{Fe} \times S_{Fe} + f_{Fe*} \times S_{Fe*} + f_{Ni*} \times S_{Ni*} + f_C \times S_C \qquad (1)$$

with S_{Fe}, S_{Fe*}, S_{Ni*} and S_C corresponding to the spectra measured on well annealed iron , on deformed iron, on deformed nickel and on pyrolythic carbon, respectively. The weighting factors (f_x) characterize the contribution of the pure elements to the fitted spectrum and, therefore, serve as chemical fingerprint. The fitting was performed in a momentum range of (5 to 35)$\times10^{-3}m_0c$.

As second method, integral parameters, so-called Shape (S) and Wing (W) parameters are determined. These parameters give information about the changes of the defect concentration (S) and can be correlated to changes of the chemical environment (W). The S parameter is assigned to the area ratio of the centre spectrum (-2.5 to 2.5)$\times10^{-3}m_0c$ and the total spectrum, whereas the W parameter is calculated by dividing the counts between electron momenta from ±(15 to 35)$\times10^{-3}m_0c$ by the total measured counts. These values are compared to the S_0 and W_0 value of the well annealed pure iron spectrum.

Studies on the microstructure were performed on samples, subjected to the same heat treatment, by optical microscopy as well as by scanning electron microscopy using an ESEM QUANTA 600 FEG.

3. Results and Discussion

3.1. Initial Condition

The meteorite sample exhibits the typical Widmanstätten structure in the cm range visible by the naked eye. Broad Ni-poor Kamacite bars are separated from fields of fine-grained Kamacite and Taenite (Plessite) by narrow bands of Ni-rich Taenite, as shown in figure 1 B. Positron lifetime measurements reveal a relatively high mean positron lifetime of 165ps. Compared to the positron lifetime in defect free iron (110 ps) [5] this shows that open volume defects are present in the meteorite sample. The lifetime of 165 ps is too short for vacancies. Typically vacancies in iron exhibit a positron lifetime of ~175 ps [5]. Due to the low cooling rate no remaining thermal vacancies are expected. This leads to the conclusion, that the positron traps in the meteorite sample are mainly dislocations.

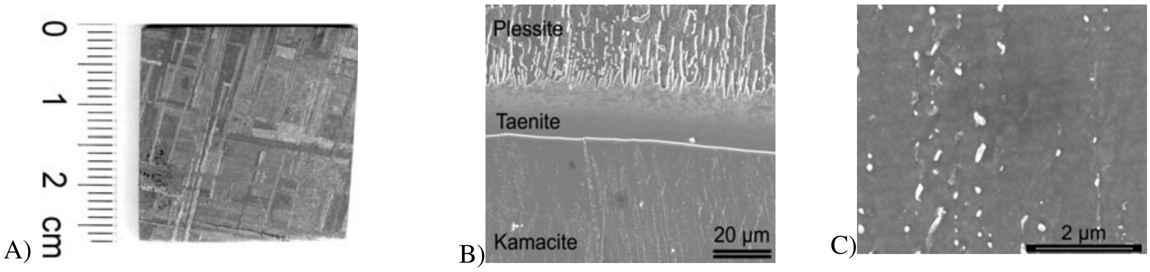

Figure 1. A) Optical micrograph of the etched meteorite surface, B) SEM micrograph and C) close up of B, showing precipitates within Kamacite bars.

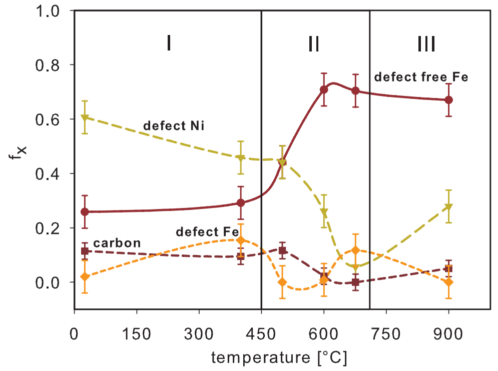

Figure 2. Evolution of the Doppler broadening fit parameter f_x (according to eq. 1) as function of annealing temperature.

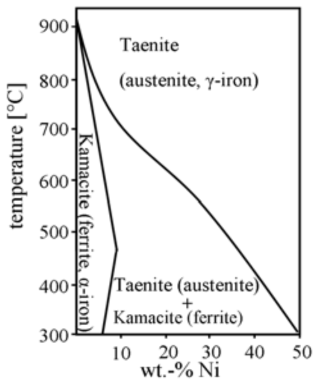

Figure 3. Fe-rich section of iron-nickel phase diagram, redrawn after [9].

With 2d-DB experiments and the numerical analysis according to eq. 1 a relatively large nickel signature is observed (Fig. 2). This indicates that misfit dislocations between the Ni-rich Taenite and Ni-poor Kamacite are present. Electron micrographs reveal that within the broad Ni-poor Kamacite bars there are small Ni-rich precipitates present (~200 nm). We, therefore, conclude that at the interface between matrix and precipitates misfit dislocations are present. In fact, the cubic base centered Kamacite (ferrite, α-iron) exhibits a lattice parameter of a = 0.286 nm and the cubic face centered, Ni-rich Taenite (austenite, γ-iron) exhibits a lattice parameter of a = 0.358 nm [7]. Furthermore, according to the phase diagram (Fig. 3) the nickel content of the Kamacite decreases after reaching a maximum at about 460°C and due to the low cooling rates and an extrapolated nickel diffusion coefficient (data from [8]) of $D \sim 1\times10^{-23}$ $m^2 s^{-1}$ at 400°C a diffusion of the nickel atoms of $\sim 3\text{x}10^{-2}$ µm/a can be estimated. Therefore, Ni-rich precipitates have to be formed during the slow cool down and in fact the misfit dislocations between the Taenite precipitates and the Kamacite matrix are found by positrons and are confirmed by electron microscopy (Fig. 1, C). In addition the numerical analysis of the 2d-DB spectra reveals a minor but detectable carbon signature. This shows that positrons are as well trapped at carbon precipitates within the meteorite sample.

3.2. Thermal Treatment

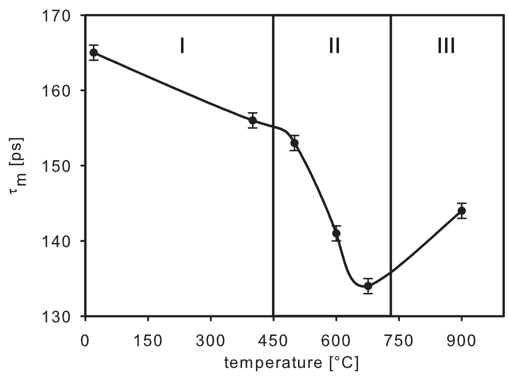

Figure 4. Mean positron lifetime τ_m as function of annealing temperature.

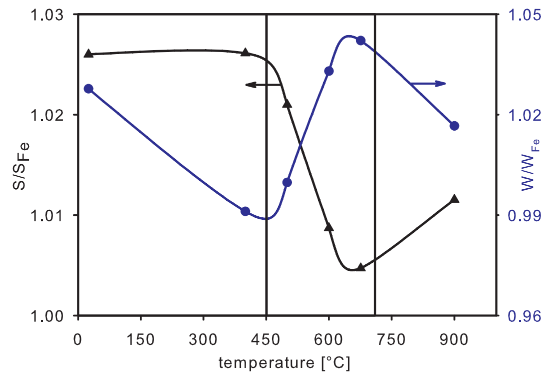

Figure 5. S- and W-Parameter as function of annealing temperature.

The meteorite samples were then subjected to subsequent isochronal thermal treatment for one hour at 400°C, 500°C, 600°C, 676°C and 900°C. The evolution of the mean positron lifetime is presented in figure 4. Upon annealing three distinct annealing stages can be observed. First, up to 400°C, a slow decrease of the mean positron lifetime can be distinguished, while the results of the Doppler broadening experiments show no decrease of the S parameter (Fig. 5) upon this temperature step. The W parameter (Fig. 5) on the other hand shows a major decrease. In addition with the numerical analysis of the 2d-DB spectra (Fig. 2) following conclusions can be drawn. Upon this temperature step the chemical environments of the open volume defects change. The nickel signature at defects decreases slightly, while the dislocations sustain. The nickel diffusion length in Fe at this temperature for one hour is approximately 0.2 nm, which is in the range of 1 lattice constant. This change of the chemical environment is as well attributed to lead to the slight decrease of the positron lifetime.

At higher temperatures, stage II, between 500°C and 676°C, the defects start to disappear, which is indicated by the strong decrease of the mean positron lifetime (Fig. 4) while at the same temperatures the S Parameter (Fig. 5) decreases rapidly as well. In addition the chemical sensitive 2d-DB spectra reveal a major increase of the pure iron signature, while the defect nickel signature decreases rapidly and the defect iron signature decreases as well (Fig. 2). The dissolution of the nickel rich precipitates at higher temperatures is confirmed by SEM micrographs. Starting at 600°C the carbon signature of the meteorite sample decreases and disappears at 676°C (Fig. 2). This incident leads to the conclusion, that carbon containing precipitates were dissolved at this temperature and the carbon now occupies interstitial sites and is not detectable by the positrons any more. The dissolution of carbon precipitates in a Fe-Ni meteorite at this temperature has in fact also been reported by Weller and Wegst [10], from internal friction experiments.

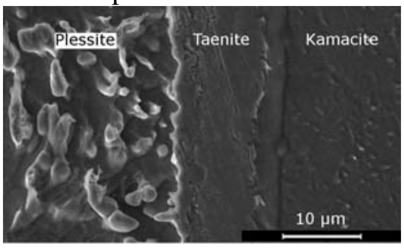

Figure 6. SEM micrograph of the Plessite, Taenite, Kamacite phase boundaries after annealing at 900°C.

Stage III, at temperatures as high as 900°C, shows a re-increase of the mean positron lifetime (Fig. 4), as well as the S parameter (Fig. 5) and indicates the formation of new open volume defects at this temperature. This and an increased contribution of the defected nickel signature of the fitting process (Fig. 2) indicate that vacancies are formed [11] and stabilised by impurity atoms. Due to the relatively short annealing times, the coarse Widmanstätten structure is still visible after annealing at 900°C. Furthermore no indications for precipitates within the Kamacite bars can be observed (Fig. 6).

4. Conclusion

It was shown, that the meteorite sample is in a stable thermodynamic equilibrium condition with respect to a) thermal vacancies and b) carbon precipitates. However, the structure of the meteorite formed upon the slow cooling exhibits the macroscopic Widmanstätten structure and c) small Ni-rich equilibrium precipitates due to the thermal decomposition of the super saturated Kamacite at low temperatures. These precipitates exhibit misfit dislocations which can be detected by positrons. The positron annihilation techniques give a comprehensive picture of the open volume defects in the meteorite sample.

References

[1] He Y, Godet S, Jacques P J and Jonas J J, 2006, *Acta Mater.* **54**, 1323
[2] Moren A E and Goldstein J I, 1978, *Earth and Planetary Science Letters* **40**, 151
[3] Puff W, Rabitsch H, Wilde G, Dinda G P and Würschum R, 2007, *J. Appl. Phys.* **101**, 123512
[4] Somoza A, Petkov M P, Lynn K G and Dupasquier A, 2002, *Phys. Rev. B* **65**, 094107
[5] Vehanen A, Hautojärvi P, Johansson J, Yli-Kauppila J and Moser P, 1982, *Phys. Rev. B* **25**, 762
[6] Okrusch M and Matthes S, 2010, *Mineralogie: Eine Einführung in die spezielle Mineralogie*, Petrologie und Lagerstättenkunde (Springer 2010)
[7] Clarke R S Jr. and Scott E R D, 1980, *Am. Mineral.* **65**, 624–630
[8] Cermak J, Lübbehusen M and Mehrer M, 1989, *Z. Metallkde.* **880**, 213
[9] Swartzendruber L J, Itkin V P and Alcock C B, 1993, in: "*Phase Diagrams of Binary Iron Alloys*", Okamoto H (ed.), Materials Information Soc., Materials Park, Ohio
[10] Weller M and Wegst U G K, 2009, *Mat. Sci. And Eng. A* **41**, 521
[11] Shirai Y, Schaefer H E, Seeger A, 1989, in: *Positron Annihilation*, World Scientific Publ. Co., Singapore, p.419